

Second-order phase transition in PbO and SnO at high pressure: Implications for the litharge-massicot phase transformation

David M. Adams, Andrew G. Christy, and Julian Haines
Department of Chemistry, University of Leicester, Leicester LE1 7RH, England

Simon M. Clark
Daresbury Laboratory, Warrington WA4 4AD, England
 (Received 13 April 1992)

We have studied the structural behavior of PbO at high pressure by powder neutron diffraction in a McWhan cell, and by energy-dispersive powder x-ray diffraction and Raman spectroscopy in a diamond anvil cell. A phase (γ -PbO) occurs at room temperature between ~ 0.7 and ~ 2.5 GPa pressure, between the stability fields of litharge (< 0.7 GPa) and massicot (2.5–10.1 GPa). There is presumably a triple point in the system at a few kbar and 0–200°C. The phase is related to litharge by a reversible second-order transition. We infer that this is associated with the collapse of the e_u acoustic mode. Unit-cell data at 1.6 GPa are $Pm2_1n$, $a = 4.027(3)$ Å, $b = 3.950(3)$ Å, $c = 4.767(4)$ Å, and $Z = 2$. The pressure evolution of the spontaneous strain follows a simple Landau model. There are four distinct solid-state transformation paths between litharge and massicot that maintain the known topotactic relationship between the phases, maintain the translational symmetry common to both, and make use of continuous transitions between group-subgroup related structural intermediates. Both the γ phase and the modulated low-temperature phase of PbO are closely related to one step on one of these paths. Although there is evidence to suggest that the intermediate states do have a transient existence, several paths appear to be utilized. A transition to a γ -like phase also occurs in SnO, at 2.5 GPa, although there is no evidence of a massicotlike polymorph of this compound. The orthorhombic phase is stable to at least 7.5 GPa.

I. INTRODUCTION

Lead oxide has long been known to occur in two polymorphs, a red tetragonal α form ($P4/mmn$, $a = 3.976$ Å, $c = 5.023$ Å, $Z = 2$) and a yellow orthorhombic β form ($Pbma$, $a = 5.489$ Å, $b = 4.755$ Å, $c = 5.891$ Å, $Z = 4$).¹ These phases occur naturally as the minerals litharge and massicot, respectively. Litharge is the stable form under ambient conditions, inverting to massicot at 1 atm, 540°C.² However, massicot shows a high degree of metastable persistence at lower temperatures. Unusually for a high-temperature phase, massicot is 3.3% denser than litharge under ambient conditions; therefore, the equilibrium line has a negative slope in P - T space. Extrapolation of the line as determined by White, Dacheville, and Roy² suggests that massicot and litharge should be in equilibrium at ~ 0.55 GPa at room temperature. The two phases are readily interconverted by grinding under ambient conditions.² The transformation appears to occur without discrete nucleation events: it is possible to generate hybrid crystals in which the phase boundaries are diffuse, and a topotactic relationship is maintained between the phases such that $[001]_\alpha \parallel [001]_\beta$, $\langle 110 \rangle_\alpha \parallel \langle 100 \rangle_\beta$, and $(010)_\beta$.¹

Recently, a low-temperature α' phase of PbO, stable below -65 °C, has been described^{3,4} whose structure is an orthorhombically distorted and incommensurately modulated variant of the litharge structure. It has been suggested by Hédoux, Gebille, and Garnier⁴ that the modulation is driven by competition between litharge and massicot structural patterns.

All of these phases possess very open structures relative to close-packed oxides. The volume per oxygen atom is 39.7 Å³ (Ref. 3) for litharge and 38.4 Å³ (Ref. 3) for massicot under ambient conditions [compare 27.5 Å³ (Ref. 3) for CaO (Ref. 5)]. The low density of the PbO phases is presumably a consequence of three interrelated factors: (i) covalent Pb-O bonding, leading to strong directionality of the Pb-O bonds and relatively low coordination numbers (4 in litharge, 2 in massicot), (ii) the low dimensionality of the structures (the primary Pb-O bonds define (001) layers in litharge, and [100] kinked chains in massicot, as can be seen in Fig. 1), and (iii) the structural roles played by the inert pair electrons of Pb. These electrons constitute a stereochemically active lone pair in litharge, projecting away from the Pb-O bonds and into the interlayer space. The 90° O-Pb-O bond angle of massicot suggests that the Pb contributions to the bonding orbitals are largely $6p$ in character, and hence the inert pair electrons are $6s$, spherical and not stereochemically active.⁶

The low density of the PbO phases at 1 bar suggests that they may transform to denser structures at relatively low pressure. We have compressed PbO in a diamond-anvil cell at room temperature and pressures up to 10.1 GPa, following the structural behavior by neutron powder diffraction,⁷ energy-dispersive x-ray powder diffraction (EDXRD), and Raman spectroscopy. A new phase, γ -PbO, was found to occur in the interval 0.7–2.5 GPa, between the litharge and massicot fields. The α - γ transition is fast, reversible, and appears to be second order. The β - γ transition is slower and not readily reversible on a laboratory timescale. Surprisingly, massicot ap-

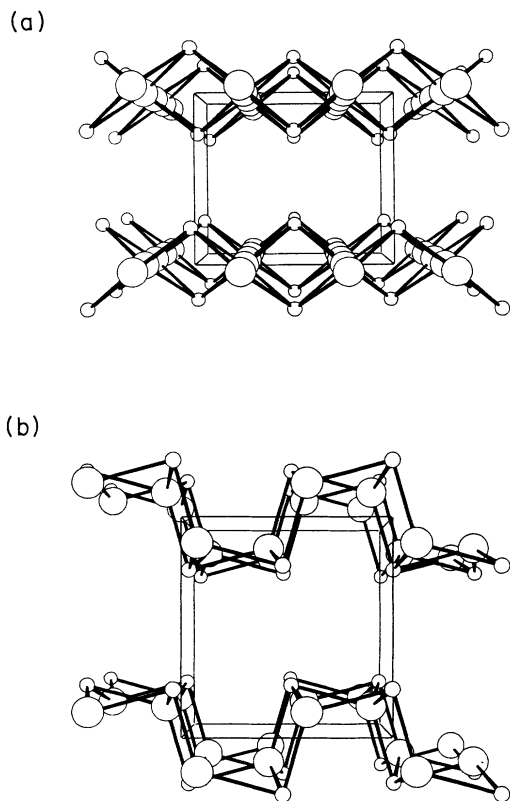


FIG. 1. The litharge (a) and massicot (b) structures, viewed down $[110]_{\alpha}$ and $[010]_{\beta}$; $[001]$ vertical for both phases.

pears to be stable up to at least 10 GPa. The new γ phase has an orthorhombic distortion of the litharge structure, oriented at 45° relative to the orthorhombic average structure of the modulated α' phase. The symmetry relationships between these and the two better known structures shed considerable light on the solid state litharge-massicot transformation mechanism. Furthermore, the observed α - γ transition pressure of ~ 0.7 GPa, and compressibility data for all three phases suggest that extrapolation of the experimental α - β line of White, Dache, and Roy² below 200°C is not valid.

SnO also has the litharge structure at ambient pressure, and has been reported to undergo a phase transition at 1.5 GPa.⁸ The transformation was described as first order, but involving a similar orthorhombic distortion to the litharge structure to that we have found for γ -PbO. We have reexamined SnO, and found a second-order transition to the corresponding phase at ~ 2.5 GPa. No indication of transition to a massicotlike phase was observed up to 7.5 GPa for SnO.

II. EXPERIMENTAL METHODS

A. Samples studied

The litharge used for this study was prepared by the method of Schoonover, Groy, and Lin.⁹ Freshly precipitated lead (II) hydroxide was dehydrated with warm 15M KOH solution, recrystallizing almost immediately into

thin red plates of litharge, some with edges exceeding 1 mm in length. A few coarse, pale yellow massicot flakes were also formed, although these were not volumetrically significant and could be separated easily by subsequent hand picking. The PbO was filtered, washed several times in water and in ethanol, and then dried.

Metastable massicot, grown hydrothermally as large single crystals by Phillips, Eindhoven⁶, was also studied from ambient pressure. The SnO used was obtained as micrometric blue-black plates of $>99\%$ purity from Aldrich Chemical Co.

B. Neutron diffraction

The unit cell of γ -PbO was obtained from a high-pressure powder neutron diffraction pattern, as reported previously.⁷ A large sample ($\sim 15\text{ mm}^3$) was placed in a cylindrical Al can with fluorinert as a hydrostatic medium, inside a McWhan-type clamped cell. The cell was then taken up to 15.8 ± 1 kbar sample pressure using a hydraulic press. Time-of-flight data were collected using the 90° diffraction angle ^3He detector bank on the Polaris instrument at the Rutherford Appleton Laboratory. The data collection time was about 12 h. A diffraction pattern was also obtained in about 2 h for litharge at ambient pressure, in a 5-mm-diam vanadium can.

C. X-ray diffraction

X-ray data were collected on the white-beam energy-dispersive station 9.7 at Daresbury Laboratory. All samples were lightly ground with internal pressure calibrants using an agate mortar and pestle, and placed in a diamond anvil cell. The gaskets used were inconel or stainless steel, preindented with sample hole diameter $\sim 200\ \mu\text{m}$. The large hole size prevented superposition of gasket diffraction peaks. Nujol was used as the quasihydrostatic pressure medium. Data collection time was 1000 sec per run, and the diffraction angle 2θ near 7° throughout. Previous experience had shown that our usual pressure calibrant, NaCl, gave diffraction peaks interfering with those of litharge at low pressure. Therefore, two other calibrants were also tried. Gold powder, with a very different lattice parameter from NaCl, avoided the interference problem but was insufficiently compressible for accurate measurement at very low pressure. KCl was used to obtain a low-pressure dataset, since it did not interfere with important litharge peaks and is very compressible. Unfortunately, KCl itself undergoes a phase transition near 2 GPa. Both Au and KCl were independently calibrated against NaCl. Pressure errors are estimated to be 0.03 GPa or less.

For some PbO samples, low-pressure diffraction patterns showed anomalous peak shapes suggestive of inhomogeneous strain in the sample. These PbO samples were rejected, and the cell reloaded with fresh PbO. The good quality of calibrant peak shapes implied that conditions in the cell were hydrostatic, and that the strain had been introduced on grinding the sample-plus-calibrant mixture. From samples giving good quality diffraction patterns, cell data were collected for α - and γ -PbO up to the point of complete conversion to massicot at ~ 3.5

GPa. A separate massicot dataset was also collected over the range 0–10.1 GPa. SnO data were collected over the range 0–7.5 GPa.

D. Raman spectroscopy

For Raman study, litharge was loaded into a diamond-anvil cell with a ruby chip as the pressure calibrant and Nujol as the pressure transmitting fluid. Spectra were obtained in backscattering mode on a Coderg T800 spectrometer using a Spectra Physics Model 164 Krypton-ion laser (647.1-nm line). The pressure was increased in small steps and data collected until the transformation to massicot was complete. A dataset for massicot was also collected from ambient up to 9.8 GPa with 16:3:1 water:methanol:ethanol as a pressure medium.¹⁰

III. RESULTS

A. Neutron diffraction

The neutron powder diffraction patterns are shown in Fig. 2 for litharge at ambient pressure, and γ -PbO at 1.6 GPa. Above the transition pressure, the litharge hhl reflections remain sharp and single, whereas the $h0l$ reflections split into two components and broaden considerably. It is possible that the broadening is caused by fine-scale twinning in the orthorhombic γ phase. The variation in peak widths prevented Rietveld refinement of the structure. Measured γ -phase peak positions from the

TABLE I. Measured and calculated d spacings for γ -PbO at 1.6 GPa.

hkl	d_{obs} (Å)	d_{calc} (Å)	$100(d_{\text{obs}}-d_{\text{calc}})/d_{\text{calc}}$
001 ^a	4.787	4.767	0.21
101	3.076	3.076	0.0
011	3.047	3.042	0.16
110	2.805	2.820	-0.53
111	2.414	2.427	-0.54
002	2.377	2.384	-0.29
102	2.085	2.051	1.66
012	2.03	2.041	-0.54
200	2.019	2.014	0.25
020	1.987	1.975	0.61
112	1.813	1.820	-0.38
211	1.680	1.679	0.06
121	1.663	1.662	0.06
003	1.588	1.589	-0.06
103	1.475	1.478	-0.21
013		1.474	0.07
220	1.403	1.410	-0.50

^aMeasured from low-angle neutron data. Not in Fig. 2.

pattern of Fig. 2 are compared with calculated positions in Table I.

B. X-ray diffraction

Cell data for all phases was refined using 6–8 fitted reflections. Parameters for the PbO α and γ phases are shown in Fig. 3, and for massicot in Fig. 4. The unit cell

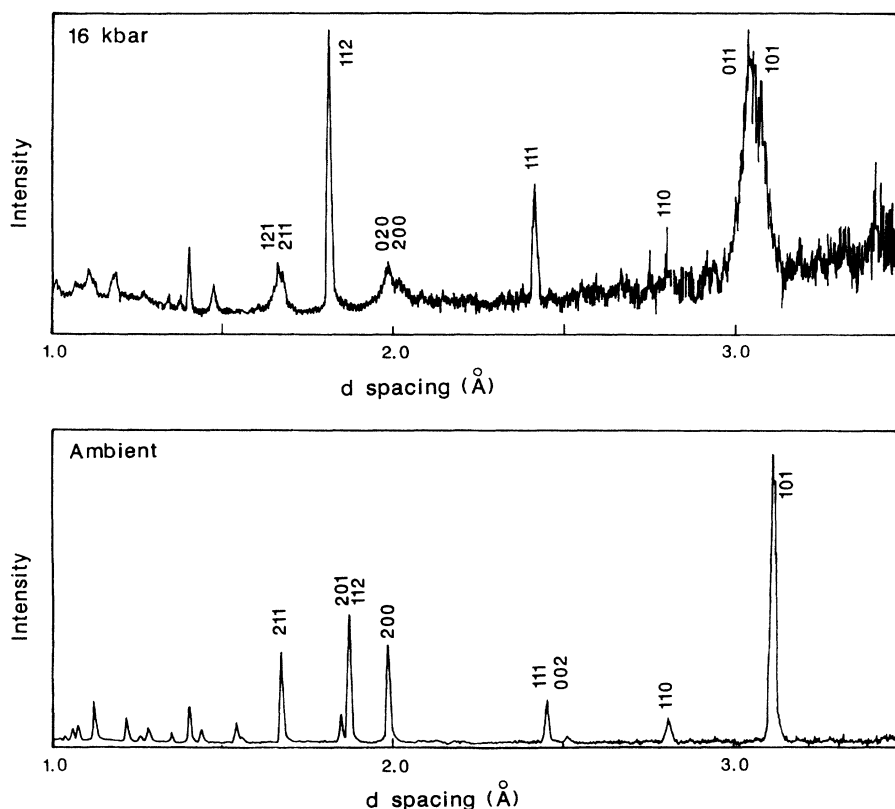


FIG. 2. Powder neutron diffraction patterns for γ -PbO (top) and litharge.

TABLE II. Cell parameters and compressibilities for PbO and SnO phases. V is the volume per formula unit. All compressibilities are pressure derivatives obtained by linear regression of refined cell parameters. The left-hand values for massicot apply over the range 0–3.5 GPa; the right-hand values are for 3.5–10.1 GPa.

Phase:	α -PbO	γ -PbO	β -PbO	α -SnO	γ -SnO
P (GPa)	0.07	2.55	0	0.13	2.57
a (Å)	3.979(3)	4.113(11)	5.499(3)	3.799(2)	3.805(28)
$a'=(a+b)/2$ (Å)		3.975(6)			3.795(15)
b (Å)		3.837(4)	4.755(3)		3.785(13)
c (Å)	5.011(7)	4.692(9)	5.906(4)	4.827(4)	4.613(13)
V (Å ³)	39.67(6)	37.02(13)	38.61(4)	34.83(3)	33.22(29)
Uniaxial and bulk compressibilities (10^{-6} GPa)					
a	55	-176	56,39	80	-163
a'		-9			-15
b		171	40,17		133
c	293	178	114,19	205	64
V	403	173	210,75	365	34

of the γ phase appears to be a simple orthorhombic distortion of the litharge phase. No evidence for superlattice or satellite reflections was seen, so we assume that the unit cell content remains the same and that the γ phase is commensurate. There is no discontinuity in lattice parameters at the transition point within experimen-

tal error, so the transition is second-order in character.

The lattice parameters of SnO up to 4.51 GPa are presented in Fig. 5. An additional EDXRD pattern collected at 7.54 GPa showed insufficient measurable peaks to be refined in the orthorhombic system, but there was no indication of another phase transition. The α - γ transition in SnO again appears to be second order, but at a

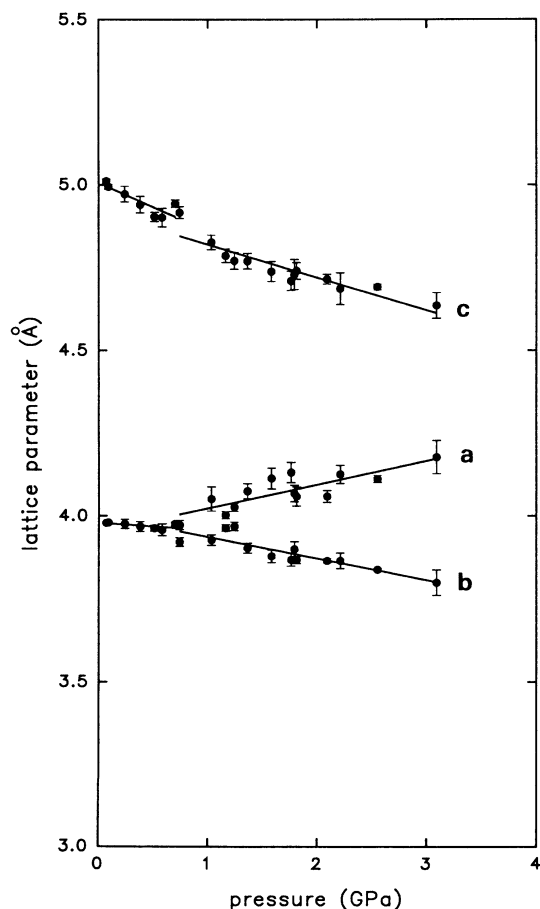


FIG. 3. Cell parameter variation with pressure for α - and γ -PbO.

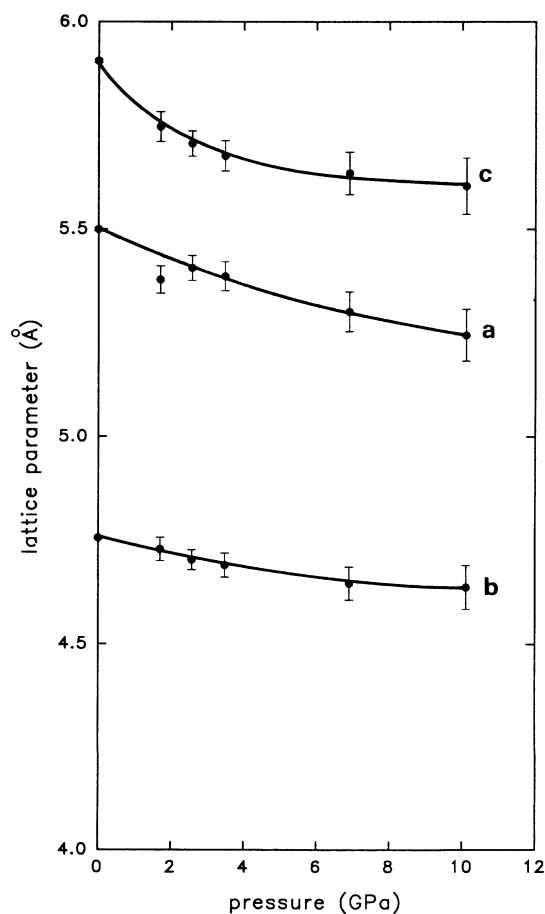


FIG. 4. Massicot cell parameters.

higher pressure than for PbO.

Cell parameters and compressibilities are shown for all phases in Table II. For the γ phases, the compressibilities are those derived from linear regression through all experimental points. The theoretical justification for linear fitting of the γ -phase parameters is discussed below. The virtual incompressibility of $(a+b)/2$ for these phases is noteworthy: all contraction of the structure in the xy plane is accomplished by orthorhombic distortion.

Volumes per formula unit are plotted for the three PbO phases in Fig. 6. It is significant that the bulk compressibility of massicot decreases rapidly with pressure, and becomes considerably less than that of the other PbO phases. The massicot data may be fit to a generalized Hook's law equation of state:

$$P = (B_0/B')[(V_0/V)^{B'} - 1],$$

giving $V_0 = 38.52 \pm 0.32 \text{ \AA}^3$, bulk modulus $B = 22.72 \pm 6.2 \text{ GPa}$, and pressure derivative $B' = 17.83 \pm 1.6$ rather than the more usual value 4–5. The compressibility at low pressure is anisotropic and mainly along the z direction (Fig. 4). The volume curves for all the other phases were too linear to fit the above equation with good constraints on B_0 and B' . They are fitted to quadratic curves in Fig.

6. Extrapolation of the litharge data suggests that at room temperature, litharge would become denser than massicot at around 2.5 GPa if the γ phase did not intervene. ΔV for this transition changes fast with pressure, so it is likely that the equilibrium line is strongly curved in P - T space, becoming closer to isothermal as P increases. This would explain the apparent incompatibility of our transition pressures with the high- T , low- P massicot-litharge line determined by White, Datchile, and Roy.² There is presumably a triple point in the system at a few kilobars pressure and 0–200°C.

C. Raman spectroscopy

Raman-active modes are shown in Fig. 7 for the α , γ , and β phases of PbO up to 5.9 kbar. We observed a marked decline in spectrum intensity at the α - γ transition, correlating with the optically observable color change from red to black. The spectra nevertheless remained of excellent quality. As massicot (visually yellow) was formed, the intensity increased again. The data of Fig. 7 were all obtained, while increasing the sample pressure. Once formed, massicot did not invert back to α - or γ -PbO on a laboratory time scale. After data collection, the sample was seen to consist completely of yellow massicot flakes freely suspended in the pressure

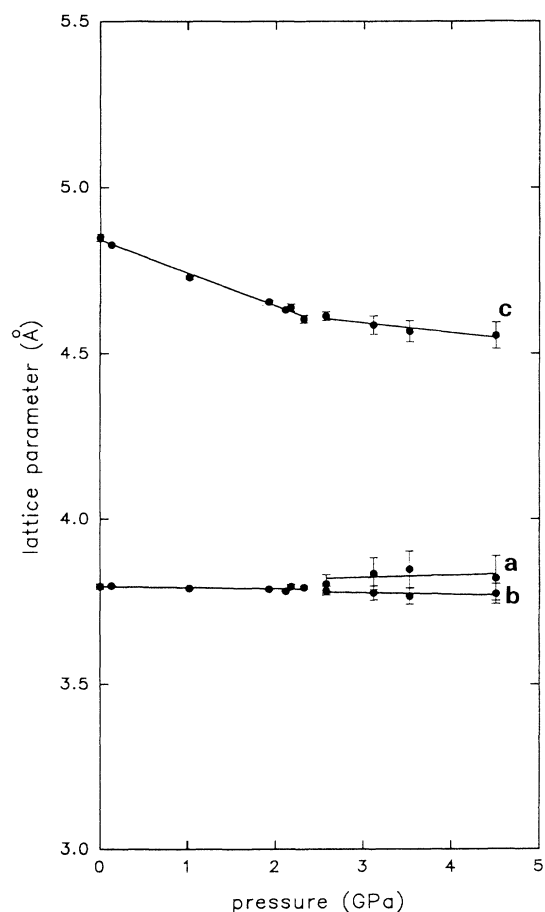


FIG. 5. SnO cell parameters.

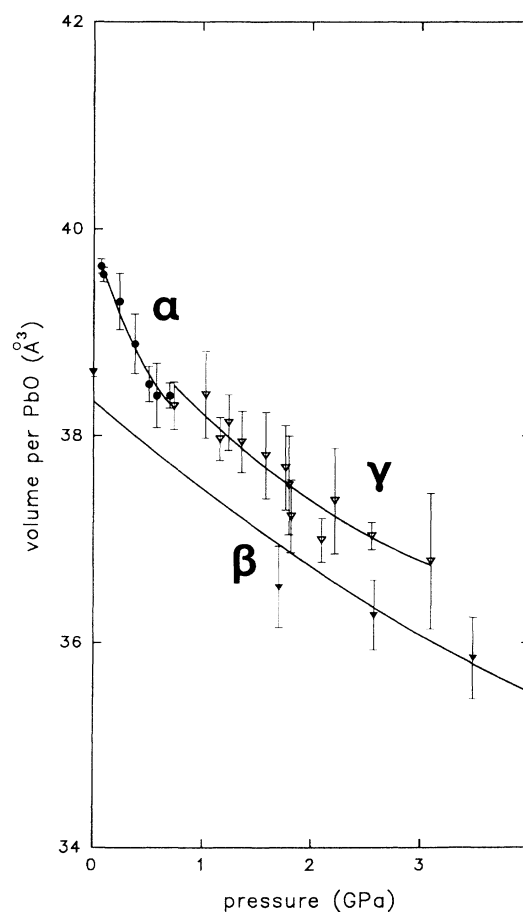


FIG. 6. Volume per formula unit for PbO phases.

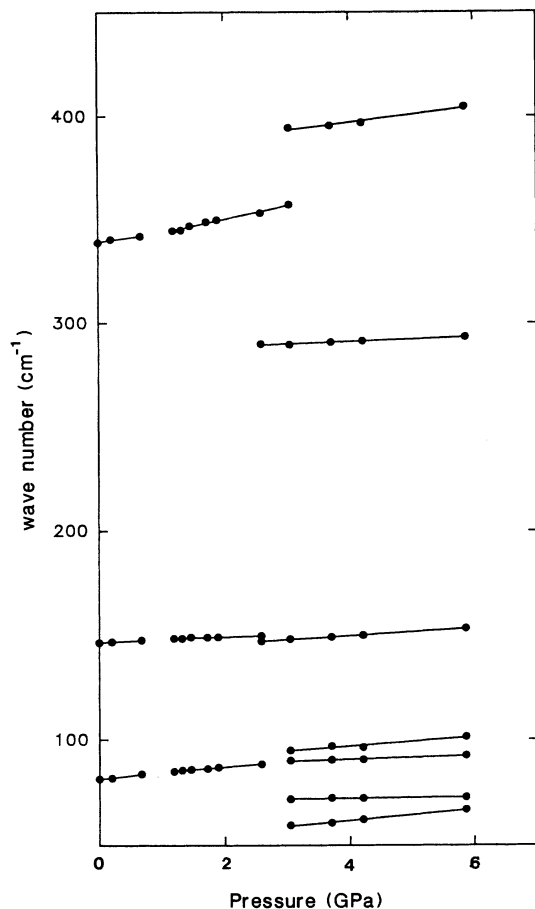


FIG. 7. Raman modes for PbO phases.

medium. The grain size suggested that the massicot flakes were transformation products of single litharge crystals.

It can be seen that the spectrum of the γ phase is very similar to that of litharge, with slight changes in slope. No splitting was resolved in the peak near 80 cm^{-1} (species e_g in litharge, as assigned by Adams and Stevens⁶). The other litharge e_g mode near 320 cm^{-1} was not observed.

All peaks in the massicot spectra corresponded to those observed and assigned by Adams and Stevens,⁶

confirming that the high-pressure transformation product of the γ phase is indeed massicot. Spectra obtained from hydrothermal massicot were identical at corresponding pressures. It is interesting to note that the 87 cm^{-1} lattice mode observed by Adams and Stevens at 1 bar resolves into two distinct modes with different pressure dependencies. All of the fundamental Raman-active modes of massicot predicted by group theory have now been accounted for. Despite the large fitted value of B' , mode frequencies varied linearly over the whole pressure range studied.

Mode frequencies and pressure shifts for all PbO phases are presented in Table III.

An important guide to the nature of the α - γ phase transition, and the space group of the γ phase, is provided by the observation that the mode near 340 cm^{-1} , unambiguously assigned as b_{1g} (Ref. 6) remains hard. The B_{1g} representation of point group $4/mmm$ transforms as $(x^2 - y^2)$, as does the orthorhombic spontaneous strain observed in the diffraction data. Therefore, if the transformation were proper ferroelastic, i.e., the spontaneous strain is a primary order parameter,¹¹ the 340 cm^{-1} mode would be expected to soften. The corresponding orthorhombic space group would be $Pmmn$, as we previously suggested before acquisition of the Raman data.⁷

The only other potential soft mode that can generate the observed distortion is the unobserved e_u acoustic mode. Acoustic-mode softening would give rise to a primary order parameter transforming as a polar vector in the (x, y) plane. In the case of this transition, the orthorhombic axes are parallel to the tetragonal axes, so either the x or the y component is constrained equal to zero. There are four twin orientations of the γ phase corresponding to polarization along $\pm x$ or $\pm y$. The corresponding space group is $P2_1mn$, or $Pm2_1n$ with interchange of x and y axes. The order parameter can be represented by its magnitude Q along the polarization direction. A look at part of the character table for $4/mmm$ at the Brillouin-zone center (Table IV) shows that

$$E_u \otimes E_u = A_{1g} + A_{2g} + B_{1g} + B_{2g} .$$

The B_{1g} spontaneous strain can therefore couple to Q^2 , and the phase transition is improper ferroelastic.¹¹ Al-

TABLE III. Raman data for PbO phases. sh is the shoulder, ν and ν_0 in cm^{-1} , and $\partial\nu/\partial P$ are in $10^{-3}\text{ cm}^{-1}\text{ GPa}^{-1}$.

α (0.2 GPa)			γ (1.2 GPa)			β (3.7 GPa)		
ν	$\partial\nu/\partial P$	ν_0	ν	$\partial\nu/\partial P$	ν_0	ν	$\partial\nu/\partial P$	ν_0
340.5	42	339.3	344.7	67	336.9	395.5	34	383.6
147.2	16	146.8	148.8	8	147.8	290.8	9	287.9
81.7	35	81.2	84.9	25	82.0	149.4	18	142.9
						97 sh	22	88.1
						90.4	9	87.3
						72.3	2	71.3
						60.4	25	51.7

TABLE IV. Partial character table for point group $4/mmm$ (D_{4h}).

rep.	pt. gp.	Multiplicity:										
		Class:	e	i	c_{2z}	m_z	c_{4z}	s_{4z}	c_{2x}	$c_{2x'}$	m_x	$m_{x'}$
A_{1g}	$4/mmm$	1	1	1	1	1	1	1	1	1	1	1
A_{2g}	$4/m$	1	1	1	1	1	1	-1	-1	-1	-1	-1
B_{1g}	mmm	1	1	1	1	-1	-1	1	-1	1	-1	-1
B_{2g}	mmm	1	1	1	1	-1	-1	-1	1	-1	-1	-1
E_u	$2mm,$ $11m$	2	-2	-2	2	0	0	0	0	0	0	0

though we have no Raman data for SnO, it is likely that the SnO transition is similar in character.

These compounds, along with paratellurite, TeO_2 ,¹² appear to be unique in showing tetragonal-orthorhombic transitions at moderate pressure, which are driven by soft acoustic modes.

IV. DISCUSSION

A. Structural model for the α - γ phase transition

In the $P4/nmm$ litharge structure, the O atoms are fixed on sites of $4m2$ symmetry (the $2a$ sites in Wyckoff notation) and the Pb atoms are free to move parallel to z , being on the $2c$ sites of $4mm$ symmetry. In the corresponding $Pm2_1n$ subgroup, all atoms are in sites of point symmetry m , and have no constraints on their y and z coordinates. The displacements away from the tetragonal coordinates are likely to be small, and the y components are constrained by the n glide to be equal in sign and magnitude for all atoms of a given type. These displacements are compatible with the adoption of a distorted zinc-blende-like structure as suggested for γ -SnO by Serebryanaya, Kabalkina, and Vereshchagin.⁸ It is evocative to notice that the extrapolated a and c parameters for γ -PbO converge symmetrically (Fig. 3 and Table I) to become equal at about 6.0 GPa ($a=c=4.40$ Å, $b=3.60$ Å, approximately). A corresponding tetragonal zinc-blende-like structure (the binary analog of the β -tin type) would have Pb-O=2.38 Å, slightly larger than in the ambient tetragonal phase (2.32 Å) and much longer than in massicot at 1 bar (2.21 Å). The γ -phase lone pairs would necessarily be stereochemically inactive and the increased Pb $6p$ character of the bonding electrons is consistent with the bond length increase. The short Pb-O distances in massicot can be rationalized in that although 90° O-Pb-O bond angles suggest zero s character for the Pb contribution to the massicot bonding orbitals, the 120° Pb-O-Pb angles imply that the oxygen contributions are sp^2 hybridized rather than sp^3 , and hence the effective oxygen radius is reduced. In the absence of a structure refinement, we hypothesize a structure for γ -PbO, which is intermediate between $B10$ (litharge structure) and tetragonally distorted $B3$ (zinc blende), as shown in Fig. 8.

B. Landau theory

The deviation of the γ phase structure from $P4/nmm$ symmetry is expressed by the magnitude of the order pa-

rameter Q . The Landau free energy of the γ phase relative to the α phase may then be expressed as a Taylor expansion, $G = \sum (a_n Q^n / n)$, where n is even, since the energy is symmetric with respect to reversal of polarization direction. The phase transition is driven by the dependence of the lowest-order term on an intensive variable, in this case pressure rather than temperature. Enumerating the first three terms, we have

$$G = \frac{1}{2}a_2(P_c - P)Q^2 + \frac{1}{4}a_4Q^4 + \frac{1}{6}a_6Q^6.$$

P_c is the critical pressure for the phase transition.

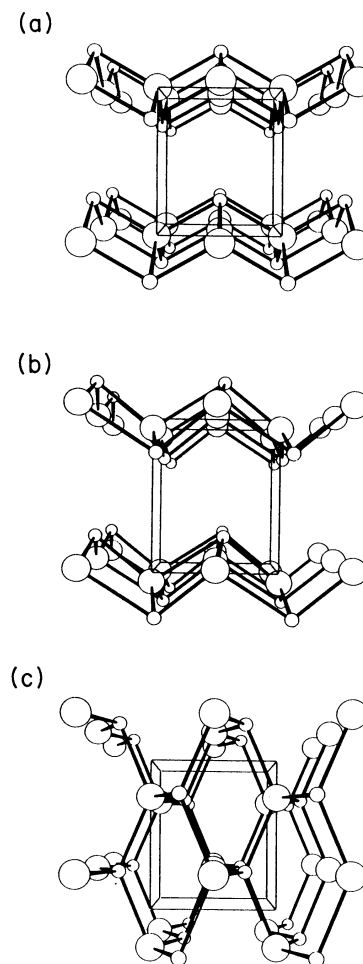


FIG. 8. (a) Litharge at ambient pressure, (b) proposed model for γ -PbO at 2.0 GPa, and (c) hypothetical β tinlike structure at 6.0 GPa.

Differentiating with respect to Q^2 , we have

$$\frac{\partial G}{\partial Q^2} = \frac{1}{2}[a_2(P_c - P) + a_4Q^2 + a_6Q^4].$$

The partial derivative in this equation is zero at equilibrium. Rearranging the equation gives

$$P = (\frac{1}{2}a_2)[a_2P_c + a_4Q^2 + a_6Q^4].$$

The spontaneous strain in the γ phase, $e_{ss} = (a - b)/(a + b)$, is likely to be closely proportional to the lowest-order term to which it couples, namely, Q^2 . Therefore, if this model of the phase transition behavior of PbO is accurate, P should be a quadratic function of e_{ss} . These two quantities are plotted against one another in Fig. 9, and it is apparent that the relationship is in fact linear, implying that a_6/a_2 is small and hence that the thermodynamics of the transition may be represented adequately without the Q^6 term. Separate regression lines are shown for the (PbO+KCl) data, since these appear to lie on a separate but parallel trend to the rest.

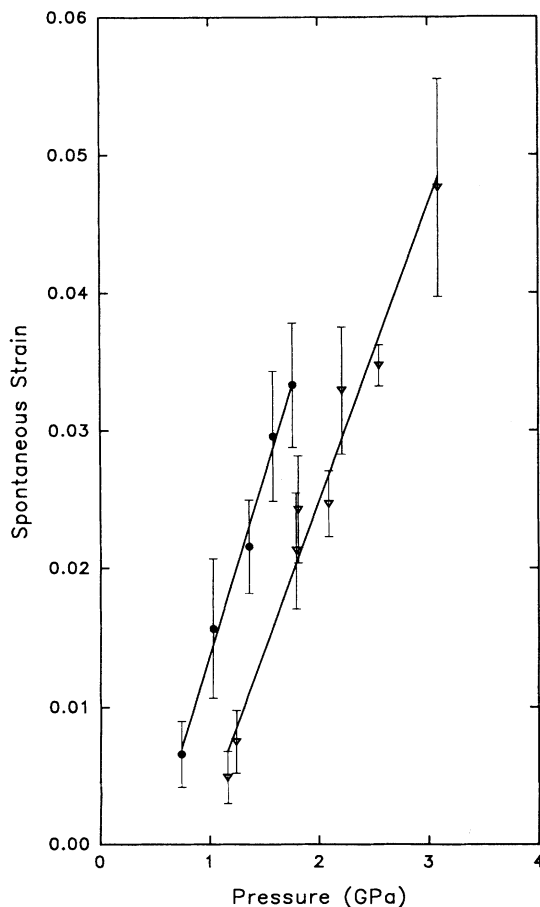


FIG. 9. Plot of spontaneous strain against pressure for γ -PbO. Lower-pressure regression line is for sample with KCl calibrant, higher pressure line for samples with Au or NaCl.

The slope a_4/a_2 is positive, since the transition is second order, and is closely similar in all cases. However, the transition pressure P_c is appreciably lower for the PbO+KCl sample (0.47 GPa) than for the other two (0.84 GPa). It is possible that the samples contain different concentrations of structure defects, and that the transition pressure varies accordingly.

C. The litharge-massicot transformation

The topotactic relationship that is often found during this transition¹ suggests that there is probably a simple set of concerted atomic movements that interconvert the litharge and massicot structures. We shall derive transformation paths between the structures using an approach inspired by Boyle, Walker, and Wanjie.¹³ In corresponding crystallographic axial settings, the space groups of litharge and massicot are $C4/amm$ and $Pbma$, respectively, $Z=4$ in both cases. Although the massicot space group is a subgroup of the litharge group, the O atoms do not lie in correlated positions in the two phases, although the Pb atoms do. Therefore, the simplest transformation routes may be found by displacing the oxygen atoms, if possible maintaining symmetric relationship between all of them and a constant unit-cell size. Continuous transformation would then be possible by moving through lower-symmetry intermediates related by group-subgroup relationships. Each massicot O position is equidistant from two possible litharge O positions. There are only two distinct ways of breaking the m planes and moving the oxygens towards litharge positions in a 1:1 fashion. Ultimately, both result in a new $Pbma$ structure, which is related to litharge by a cell-doubling (M -point) transition. Consideration of small displacements of the litharge oxygens from their ideal positions leads to the other routes seen with these in Fig. 10. The active irreducible representations involved in all three initial steps away from litharge are doubly degenerate because the tetrad axis is lost at this step and there is ambiguity about the choice of x and y axes. All the other transitions make use of one-dimensional representations.

Thus, there are four distinct three-step paths from litharge to massicot or vice versa. Which, if any of them, are utilized during the transformation? The $Cm2a$ structure is derived from $C4/amm$ via the E_u representation at the zone center. That is, the same representation as is used in generating the γ phase from litharge, but with the orthorhombic axes oriented at 45° to those of the γ phase. The symmetry is the same as that of the average structure of the low-temperature α' phase,^{3,4} although in that phase the acoustic mode collapses at a point removed from the zone center, and the crystal is modulated normal to the m plane. In symmetry terms, both the γ and α' phases can be regarded as frozen-out intermediate states on the same transformation path between litharge and massicot. Interestingly, Schoonover, Groy, and Lin⁹ reported the splitting of massicot x-ray diffraction peaks into several distinct maxima during solid-state transformation between litharge and massicot, the composite peak profiles varying as the transformation proceeded.

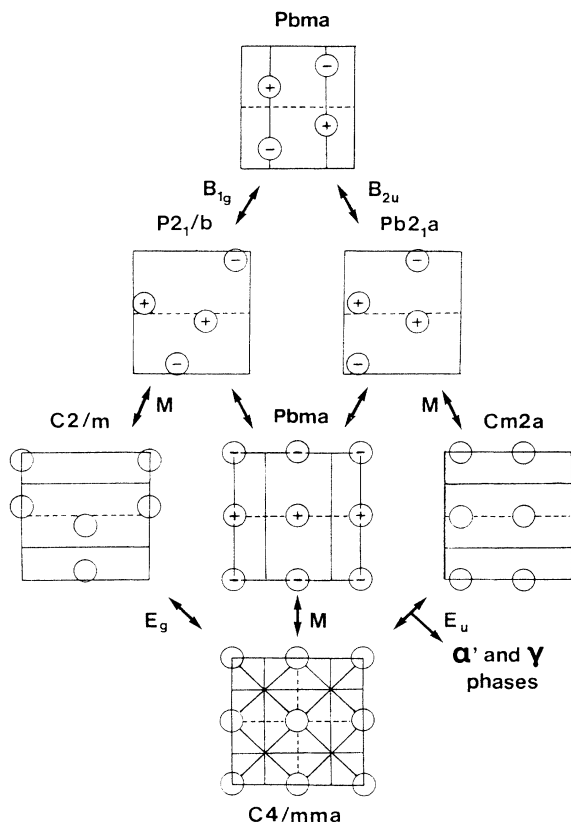


FIG. 10. The transformation paths between litharge (bottom) and massicot (top). Oxygen atoms only are shown, displacement above or below the plane of the paper being indicated by + or -, respectively. Space groups and active irreps of the higher symmetry phases are indicated, as are vertical mirror and glide planes for orientation.

In particular, the splitting of the massicot $\{111\}$ reflection in the diffraction patterns of Ref. 9 implies diffraction from more than one domain with different sets of orthorhombic cell parameters or with symmetry lower than orthorhombic. This suggests that diffracting domains of the metastable states of Fig. 10 occur during the transformation. However, the peak profiles appear too complex for the $Cm2a$ path to be used exclusively.

D. Structural behavior in related compounds

The massicot structure appears to be unique to PbO at present. It is interesting to note that the a and c parameters approach one another at high pressure. This brings about an increasing resemblance between the (010) planes of massicot and corresponding planes in the NaCl structure. A transformation to the NaCl structure could be easily accomplished by shear of such planes parallel to $\pm x$. Adoption of the NaCl structure would bring PbO into line with the heavier chalcogenides PbS, PbSe, and PbTe, all of which have this structure at 1 bar, and then successively transform into TII/SnS-like and CsCl-like structures at higher pressures.^{14,15} There are interesting

implications for the stereoactivity of the lone pair as a function of pressure. In the established phases of PbO, the lone pair shows strong localization initially (litharge) and becomes inactive once transformation into the massicot structure occurs. In the PbS phase sequence, the lone pair is initially inactive (galena, $B1$ structure), and is so again above 215 kbar ($B2$ structure). However, the intermediate TII-type phase is characteristic of binary compounds containing at least one highly polarizable or intrinsically nonspherical species (OH^- , SH^- , I^-).^{16,17} It is likely that the atom in question in Pb(S,Se,Te) is Pb. The nature of the Pb- X bonding in these compounds also appears to vary with pressure in a complex fashion and is not directly related to lone pair behavior. Band-gap closure and reopening for PbO is implied by the color changes $\alpha(\text{red}) \rightarrow \gamma(\text{black}) \rightarrow \beta(\text{yellow})$. Likewise, although PbS and PbSe are narrow-gap semiconductors at ambient, and PbTe a metal, Chattopadhyay, Werner, and von Schnering¹⁴ note that calculated $r_\sigma - r_\pi$ bond orbital coordinates suggest an increase in covalency in the TII-like phases.

A need for caution in making general predictions about other systems is indicated by the very different behavior of the group-I iodides. CuI and AgI are of considerable interest in that both have (different) fast-ion conductor phases at easily accessible temperatures. Both also appear to have low-temperature (200°C) high-pressure antilitharge phases,^{18,19} between zinc blende and NaCl structure stability fields, rather than at lower densities than either, as the behavior of PbO would suggest.

V. SUMMARY

The tetragonal litharge structures of both PbO and SnO undergo phase transitions to orthorhombically distorted variants at 0.7 GPa and 2.5 GPa, respectively at room temperature. The transitions are second order and reversible for both compounds. In the case of PbO, a further transformation to the massicot structure begins at 2.5 GPa, which is slow and irreversible on a laboratory timescale. No further transitions were seen for SnO up to 7.5 GPa.

No softening of the Raman-active b_{1g} mode was observed for PbO. In conjunction with the linear pressure evolution of the cell parameters in the new orthorhombic phase, this indicates that the transition is driven by softening of an e_g acoustic mode at the Brillouin-zone center, leading to electric polarization of the structure along one of the $\langle 100 \rangle_{\text{tetr}}$ directions. The transformation is improper ferroelastic, since the spontaneous strain couples to the square of the polarization.

Softening of the litharge e_g mode away from the zone center at low-temperature accounts for the formation of the modulated α' phase below -65°C . Thus, the new γ phase and the α' phase are formed from litharge by similar mechanisms.

It is possible to construct four interlinked diffusionless transformation paths between litharge and massicot using only three steps in each case (an infinitude of more com-

plex paths could be constructed). Each step on such a path is a potentially continuous transformation between structural states of distinct symmetries, which may be either transient intermediates or phases that are macroscopically observable. The γ phase of PbO is a thermodynamically stable instance of a phase predicted to occur on one of the litharge-massicot transformation paths.

ACKNOWLEDGMENTS

This work was supported by the Science and Engineering Council of Great Britain. J.H. acknowledges the financial support of the NSERC, Canada. We would like to thank Dr. S. Hull (RAL) for his assistance with the neutron work.

-
- ¹R. Söderquist and B. Dickens, *J. Phys. Chem. Solids* **28**, 823 (1967).
- ²W. B. White, F. Dachele, and R. Roy, *J. Am. Ceram. Soc.* **44**, 170 (1961).
- ³J. Moreau, J. M. Kiat, P. Garnier, and G. Calvarin, *Phys. Rev. B* **39**, 10 296 (1989).
- ⁴A. Hédoux, D. Grebille, and P. Garnier, *Phys. Rev. B* **40**, 10 653 (1989).
- ⁵R. W. G. Wyckoff, *The Structure of Crystals* (The Chemical Catalog Company, Inc., New York, 1931).
- ⁶D. M. Adams and D. C. Stevens, *J. Chem. Soc. Dalton* **1977**, 1097 (1977).
- ⁷D. M. Adams, A. G. Christy, and J. Haines (unpublished).
- ⁸N. R. Serebryanaya, S. S. Kabalkina, and L. F. Vereshchagin, *Dokl. Akad. Nauk SSSR* **14**, 307 (1969) [*Sov. Phys. Dokl.* **14**, 672 (1970)].
- ⁹J. R. Schoonover, T. L. Groy, and S. H. Lin, *J. Solid State Chem.* **83**, 207 (1989).
- ¹⁰I. Fujishiro, G. J. Piermarini, S. Block, and R. G. Munro (unpublished).
- ¹¹E. K. H. Salje, *Phase Transitions in Ferroelastic and Coelastic Crystals*, Cambridge Topics in Mineral Physics and Mineral Chemistry, Vol. 1 (Cambridge University Press, Cambridge, England, 1990).
- ¹²D. M. Adams and S. K. Sharma, *J. Phys. Chem. Solids* **39**, 515 (1978).
- ¹³L. L. Boyle, J. R. Walker, and A. C. Wanjie, *Faraday Discussions* **69**, 115 (1980).
- ¹⁴T. Chattopadhyay, A. Werner, and H. G. von Schnering, *Mater. Res. Soc. Symp. Proc.* **22**, 93 (1984).
- ¹⁵T. Chattopadhyay, H. G. von Schnering, W. A. Grosshans, and W. B. Holzapfel, *Physica* **139&140B**, 356 (1986).
- ¹⁶D. M. Adams, A. G. Christy, and J. Haines, *J. Phys. Chem.* (to be published).
- ¹⁷Julian Haines and Andrew G. Christy, *Phys. Rev. B* **46**, 8797 (1992).
- ¹⁸S. Hull, D. A. Keen, and R. L. McGreevy, Rutherford Laboratory Report No. RAL-91-089 (1991).
- ¹⁹V. Meisalo and M. Kalliomäki, *High Temp. High Press.* **5**, 663 (1973).